Available online at www.sciencedirect.com
SCIENCE DIRECT®
Journal of Solid State Chemistry 179 (2006) 2367–2375
JOURNAL OF SOLID STATE CHEMISTRY
www.elsevier.com/locate/jssc

Self-assembly of four new extended architectures based on reduced polyoxometalate clusters and cadmium complexes

Ying Ma, Yangguang Li, Enbo Wang*, Ying Lu, Xinlong Wang, Xinxin Xu

Department of Chemistry, Institute of Polyoxometalate Chemistry, Northeast Normal University, Changchun 130024, PR China

Received 17 January 2006; received in revised form 3 April 2006; accepted 12 April 2006
Available online 4 May 2006

Abstract

Four new $[P_4Mo_6]$ cluster-based extended structures containing cadmium complexes, $[Cd_3(4,4'\text{-Hbpy})_2(4,4'\text{-bpy})_2(H_2O)_8][Cd(H_2PO_4)_2(HPO_4)_4(PO_4)_2(MoO_2)_{12}(OH)_6]\cdot 7H_2O$ **1**, $(4,4'\text{-Hbpy})_2[Cd(4,4'\text{-bpy})_3(H_2O)_3][Cd(4,4'\text{-bpy})(H_2O)]_2[Cd(H_2PO_4)_2(HPO_4)_4(PO_4)_2(MoO_2)_{12}(OH)_6]\cdot H_2O$ **2**, $[Cd_4(phen)_2(H_2O)_4][Cd(phen)(H_2O)]_2[Cd(HPO_4)_4(HPO_4)_4(MoO_2)_{12}(OH)_6]\cdot 5H_2O$ **3** and $[Cd_4(2,2'\text{-bpy})_2(H_2O)_4][Cd(2,2'\text{-bpy})(H_2O)]_2[Cd(HPO_4)_4(HPO_4)_4(MoO_2)_{12}(OH)_6]\cdot 3H_2O$ **4** (4,4′-bpy = 4,4′-bpyridine, phen = 1,10-phenanthroline, 2,2′-bpy = 2,2′-bpyridine), have been synthesized and characterized by elemental analysis, IR, TG and single crystal X-ray diffraction. The structure of compound **1** is constructed from the $Cd[P_4Mo_6]_2$ dimers linked by $[Cd_3(4,4'\text{-Hbpy})_2(4,4'\text{-bpy})_2(H_2O)_8]$ subunits to generate a plane layer. Compound **2** consists of the positive 2D sheets that constructed from $Cd[P_4Mo_6]_2$ dimers linked by $[Cd(4,4'\text{-bpy})(H_2O)]$ complexes, then the 2D sheets are further linked up together to form a 3D supramolecular framework via extensive hydrogen-bonding interactions among the $[P_4Mo_6]$ clusters, free 4,4′-bpy molecules, dissociated $[Cd(4,4'\text{-bpy})_3(H_2O)_3]^{2+}$ complexes and water molecules. Compounds **3** and **4** show new 2D layered structure, with $Cd[P_4Mo_6]_2$ building blocks connected by tetra-nuclear $[Cd_4\{(phen)_2/(2,2'\text{-bpy})_2\}(H_2O)_4]$ clusters and $[Cd(phen/2,2'\text{-bpy})(H_2O)]$ complexes. The fluorescent activities of compounds **3** and **4** are reported.

Keywords: Polyoxometalates; Transition metal complexes; Cadmium; Crystal structure; Hydrothemal synthesis

1. Introduction

Polyoxometalates (POMs) are a well-known class of metal-oxide clusters. Considerable attention has been focused on this kind of metal-oxide-based solid materials due to their potential applications in catalysis, sorption, optical material, eletrochromism, magnetism and medicine, as well as the diversity of their structures [1]. The evolution of polyoxometalate chemistry is dependent on the design and synthesis of new materials possessing unique structures and properties [2]. One kind of promising strategy is to connect polyoxometalate building units with secondarily transition metal complexes via covalent bonds. The transition metal complexes can dramatically influence the inorganic oxide microstructure, so we can combine the merit of POMs and transition metal complexes to constitute some interesting compounds with unique properties [3].

In the field of POMs, reduced molybdenum phosphates constitute a large class of compounds and received much attention for their applications in catalysis, ion exchange, and molecular sieves [4]. The $[P_4Mo_6O_{28}(OH)_3]^{9-}$ anion (denoted $[P_4Mo_6]$), with various degrees of protonation is the most often encountered building unit in the reduced molybdenum phosphates. In the reported reduced molybdenum phosphates, $[P_4Mo_6]$ building units mostly were linked by alkali metal cations or first row transition metal cations to form 1D polymers or 2D and 3D microporous or tunnel materials [5–21]. However, the examples of reduced molybdenum phosphates connected with transition metal complexes have rarely been reported [13,17–19,21,23]. On the other hand, we noticed that the number of this kind of POMs supported by second row transition metal was even more rare [22]. Therefore, we are interested in the assembly of reduced phosphomolydates in the presence of Cd^{2+} and

*Corresponding author. Fax: +86 431 5098787.
E-mail address: wangenbo@public.cc.jl.cn (E. Wang).

0022-4596/$ - see front matter © 2006 Elsevier Inc. All rights reserved.
doi:10.1016/j.jssc.2006.04.031

organic ligands under the hydrothermal condition, and expect to obtain some novel solid-state materials with reduced molybdenum phosphates as building units and cadmium coordination complexes as linkers.

Furthermore, in all the reported work based on $[P_4Mo_6]$ clusters combined with transition metal complexes, the organic components are fully concentrated on the chelate ligands, such as 2,2′-bpy or phen. However, the polyfunctional linear ligands such as 4,4′-bpy are never grafted into the backbone of reduced molybdenum phosphates. So we chose 4,4′-bpy as organic component and successfully prepared two novel compounds $[Cd_3(4,4'\text{-Hbpy})_2(4,4'\text{-bpy})_2(H_2O)_8][Cd(H_2PO_4)_2(HPO_4)_4(PO_4)_2(MoO_2)_{12}(OH)_6]\cdot 7H_2O$ **1** and $(4,4'\text{-Hbpy})_2[Cd(4,4'\text{-bpy})_3(H_2O)_3][Cd(4,4'\text{-bpy})(H_2O)]_2[Cd(H_2PO_4)_2(HPO_4)_4(PO_4)_2(MoO_2)_{12}(OH)_6]\cdot H_2O$ **2**. In addition, to date there is no report on the luminescent properties of cadmium-linked reduced molybdenum phosphates, although they may possess potential luminescent activity. Thus we adopted Cd–phen and Cd–2,2′-bpy complexes as the linkers to constructed reduced molybdenum phosphates and successfully synthesized compounds $[Cd_4(phen)_2(H_2O)_4][Cd(phen)(H_2O)]_2[Cd(HPO_4)_4(HPO_4)_4(MoO_2)_{12}(OH)_6]\cdot 5H_2O$ **3** and $[Cd_4(2,2'\text{-bpy})_2(H_2O)_4][Cd(2,2'\text{-bpy})(H_2O)]_2[Cd(HPO_4)_4(HPO_4)_4(MoO_2)_{12}(OH)_6]\cdot 3H_2O$ **4**. The four compounds are built of $Cd[P_4Mo_6]_2$ dimers as the basic structural motif. The structure of compound **1** is constructed from the $Cd[P_4Mo_6]_2$ dimers linked by $[Cd_3(4,4'\text{-Hbpy})_2(4,4'\text{-bpy})_2(H_2O)_8]$ subunits to generate a plane layer. Compound **2** consists of the positive 2D sheets that are constructed from $Cd[P_4Mo_6]_2$ dimers linked by $[Cd(4,4'\text{-bpy})(H_2O)]$ complexes. Then the 2D sheets are further linked up together to form a 3D supramolecular framework via extensive hydrogen-bonding interactions among the $[P_4Mo_6]$ clusters, free 4,4′-bpy molecules, dissociated $[Cd(4,4'\text{-bpy})_3(H_2O)_3]^{2+}$ complexes and water molecules. Compounds **3** and **4** show new 2D layered structure, with $Cd[P_4Mo_6]_2$ building blocks connected by tetra-nuclear $[Cd_4\{(phen)_2/(2,2'\text{-bpy})_2\}(H_2O)_4]$ clusters and $[Cd(phen/2,2'\text{-bpy})(H_2O)]$ complexes. To the best of our knowledge, compounds **1**–**4** represent the first examples of 2D reduced cadmium molybdenum (V) phosphates. Furthermore, the fluorescent activities of compounds **3** and **4** are reported.

2. Experimental

2.1. General procedures

All chemicals purchased were of reagent grade and used without further purification. Elemental analyses (C, H and N) were performed on a Perkin-Elmer 2400 CHN elemental analyzer. The content of Cd, Mo and P were determined by a Leaman inductively coupled plasma (ICP) spectrometer. FTIR spectra were recorded in the range 4000–400 cm^{-1} on an Alpha Centaurt FTIR spectrophotometer using a KBr pellet. TG analyses were performed on a Perkin-Elmer TGA7 instrument in flowing N_2 with a heating rate of 10 °C min^{-1}. Photoluminescence spectra were measured using a FL-2T2 instrument (SPEX, USA) with 150 W Xenon lamp monochromatized by double grating (1200). X-ray power diffraction (XPRD) patterns were recorded on a Simens D5005 diffractometer with Cu$K\alpha$ ($\lambda = 1.5418$ Å) radiation.

2.2. Hydrothermal synthesis

Compound **1** was synthesized from a mixture of MoO_3 (0.3 mmol), $Cd(OAc)_2\cdot 2H_2O$ (0.6 mmol), D, L-α-alanine (0.9 mmol), 4,4′-bipy (0.6 mmol), H_3PO_4 (0.3 mL) and 5 mL of H_2O. The starting pH value was adjusted to 4.5 by the addition of 1 M NaOH and the mixture was stirred for 20 min in air. After that, the reagents were transferred to a Teflon-lined autoclave (20 mL) and kept at 170 °C for 5 days. After slow cooling at a rate of 10 °C/h to room temperature, orange block-like crystals were filtered off together with a small quantity of red single crystals of **2** and amorphous black powers which cannot be unidentified, then washed with distilled water and dried in a desiccator at room temperature (yield: 34% based on Mo). The ICP analysis showed that compound **1** contained Mo, 30.62%; Cd, 11.91%; P, 6.52% (calcd: Mo, 30.67%; Cd, 11.98%; P, 6.60%). The elemental analysis found: C, 12.85%; H, 2.19%; N, 3.20% (calcd.: C, 12.80%; H, 2.15%; N, 2.99%).

An identical procedure with **1** was followed to prepare **2** except the starting pH value was changed from 4.5 to 5.0. Red block-like crystals were filtered off together with a small quantity of amorphous black powers, then washed with distilled water and dried in a desiccator at room temperature (yield: 51% based on Mo). The ICP analysis showed that compound **2** contained Mo, 28.39%; Cd, 11.05%; P, 6.14% (calcd.: Mo, 28.37%; Cd, 11.08%; P, 6.11%). The elemental analysis found: C, 20.75%; H, 2.12%; N, 4.86% (calcd.: C, 20.72%; H, 2.09%; N, 4.83%).

The preparation of **3** and **4** were identical with **1** except 4,4′-bpy was replaced by phen for **3** and 2,2′-bpy for **4**, as well as the starting pH was changed to 3.0. Orange block-like crystals of **3** were filtered off together with a small quantity of amorphous black powers, then washed with distilled water and dried in a desiccator at room temperature (yield: 56% based on Mo). The ICP analysis showed that compound **3** contained Mo, 28.09%; Cd, 19.11%; P, 6.08% (calcd.: Mo, 28.03%; Cd, 19.16%; P, 6.03%). The elemental analysis found: C, 14.08%; H, 1.56%; N, 2.79% (calcd.: C, 14.04%; H, 1.57%; N, 2.73%). Orange plate-like crystals of **4** were filtered off together with a small quantity of amorphous black powers, then washed with distilled water and dried in a desiccator at room temperature (yield: 58% based on Mo). The ICP analysis showed that compound **4** contained Mo, 28.92%; Cd, 19.83%; P, 6.26% (calcd.: Mo, 28.96%; Cd, 19.80%; P, 6.23%). The elemental analysis found: C, 12.12%; H, 1.58%; N, 2.89% (calcd.: C, 12.09%; H, 1.52%; N, 2.82%).

Table 1
Crystal data and structure refinement for **1**, **2**, **3** and **4**

	1	**2**	**3**	**4**
Empirical formula	$C_{40}H_{80}Cd_4Mo_{12}N_8O_{77}P_8$	$C_{70}H_{84}Cd_4Mo_{12}N_{14}O_{68}P_8$	$C_{48}H_{64}Cd_7Mo_{12}N_8O_{73}P_8$	$C_{40}H_{60}Cd_7Mo_{12}N_8O_{71}P_8$
F_w	3753.76	4058.15	4106.91	3974.80
Crystal system	Triclinic	Monoclinic	Triclinic	Triclinic
Space group	*P*−1	*C2/c*	*P−1*	*P*−1
a (Å)	13.614(3)	28.525(6)	12.948(3)	12.892(3)
b (Å)	14.051(3)	16.354(3)	13.289(3)	13.339(3)
c (Å)	14.804(3)	24.075(5)	16.106(3)	15.456(3)
α (°)	104.62(3)	90	70.55(3)	69.04(3)
β (°)	108.44(3)	100.24(3)	70.09(3)	70.92(3)
γ (°)	105.08(3)	90	79.81(3)	80.84(3)
V (Å^3)	2414.7(8)	11052(4)	2232.1(8)	2343.0(8)
Z	1	4	1	1
μ (mm^{-1})	2.616	2.292	3.210	3.350
T (K)	293(2)	293(2)	293(2)	293(2)
λ (Å)	0.71073	0.71073	0.71073	0.71073
Final R_1, wR_2 [$I>2\sigma(I)$]	0.0376, 0.1610	0.0700, 0.1241	0.0500, 0.1891	0.0339, 0.0849
Final R_1, wR_2 (all data)	0.0423, 0.1666	0.0909, 0.1304	0.0665, 0.1991	0.0370, 0.0863

Note: $R1 = \sum\|F_o\|-\|F_c\|/\sum|F_o|$; $wR_2 = \sum[w(F_o^2-F_c^2)^2]/\sum[w(F_o^2)^2]^{1/2}$.

2.3. X-ray crystallography

Crystal data for compounds **1**–**4** were collected on a Rigaku *R*-axis RAPID IP diffractometer at 293 K using graphite-monochromated Mo*K*α radiation ($\lambda = 0.71073$ Å) Empirical absorption correction was applied. The structures were solved by the direct method and refined by the full-matrix least-squares method on F^2 using the SHELXTL 97 crystallographic software package [23]. Anisotropic thermal parameters were used to refine all non-hydrogen atoms in **1**–**4**. In **1**, **3** and **4**, the hydrogen atoms attached to carbon atoms were fixed in ideal positions and other hydrogen atoms were not located. In **2** only positions of the hydrogen atoms attached to O1W and O2W were located from difference maps; and those attached to other water molecules were not located. The hydrogen atoms attached to the carbon atoms were fixed in ideal positions, and the other hydrogen atoms were not located in **2**. A summary of the crystallographic data and structural determination for **1**–**4** are provided in Table 1.

3. Results and discussion

3.1. Structure description

Single-crystal X-ray diffraction analysis was performed on **1**–**4**; the basic building unit in the structure of the five compounds is the $[P_4Mo_6]$. As is usually observed, $[P_4Mo_6]$ is made up of six MoO_6 octahedra and four PO_4 tetrahedra. The six oxo-bridged molybdenum atoms (Mo–O: 1.667–2.336 Å for **1**, 1.673–2.350 Å for **2**, 1.670–2.324 Å for **3**, 1.667–2.307 Å for **4**) are coplanar and constitute a hexametric molybdenum cluster with alternating Mo–Mo (ca. 2.60 Å for **1**, 2.63 Å for **2**, 2.61 Å for **3**, 2.61 Å for **4**) bonds and non-bonding Mo–Mo contacts (ca. 3.55 Å for **1**, 3.54 Å for **2**, 3.55 Å for **3**, 3.53 Å for **4**). The central PO_4 group provides three oxygen atoms that bridge the bonding Mo–Mo contacts, while each of the remaining three PO_4 groups has two oxygen atoms to span the non-bonding Mo–Mo contacts. The P–O bond length is in the range of 1.490(5)–1.569(5) Å for **1**, 1.484(6)–1.594(5) Å for **2**, 1.509(7)–1.567(8) Å for **3** and 1.503(5)–1.571(5) Å for **4**. Valence bond calculations [24] not only confirm that all Mo atoms are in reduced oxidation state (+5), Cd atoms are +2, but also show the μ_2–O atoms between non-bonding Mo atoms (O22, O23, O25 for **1**, O11, O26, O31 for **2**, O4, O5, O14 for **3**, O3, O25, O31 for **4**) and part of P–O groups (O2, O3, O4, O5 for **1**, O1, O5, O10, O24 for **2**, O18, O23 for **3**, O8, O14 for **4**) are protonated. The molybdenum hexamer thus can be formulated as $[(H_2PO_4)(HPO_4)_2(PO_4)(MoO_2)_6(OH)_3]^{5-}$ for **1** and **2**, $[(HPO_4)_2(PO_4)_2(MoO_2)_6(OH)_3]^{7-}$ for **3** and **4**. In **1**–**4**, a Cd^{2+} ion is regular octahedral coordination and bridges two $[P_4Mo_6]$ units into a dimer via three μ_3–O atoms, which link the metal–metal bonded molybdenum atoms together to form a centrosymmetrical $Cd[P_4Mo_6]_2$ cluster unit (as shown in Figs. 1, 3, 6a and 8a).

The structure of **1** was constructed from $Cd[P_4Mo_6]_2$ dimers bonded together with octahedral Cd^{2+} into a 2D framework. There are three crystallographically independent Cd atoms in compound **1** (see Fig. 1): Cd(1) is located in the $Cd[P_4Mo_6]_2$ dimers and bridges two $[P_4Mo_6]$ units via three μ–O atoms (O31, O28, O26), which link the metal–metal-bonded molybdenum atoms together with Cd–O bond at lengths of 2.233(4) Å × 2, 2.287(4) Å × 2, 2.297(4) Å × 2 to form centrommetric $Cd[P_4Mo_6]_2$ dimers. Cd(2) is coordinated with a nitrogen atom (N4B) of a 4,4′-bpy molecule, two oxygen atoms (O19 and O30) of a $[P_4Mo_6]$ cluster and two water molecules (O3W and O4W). Cd(3) is defined by two nitrogen atoms (N1 and N2) of two

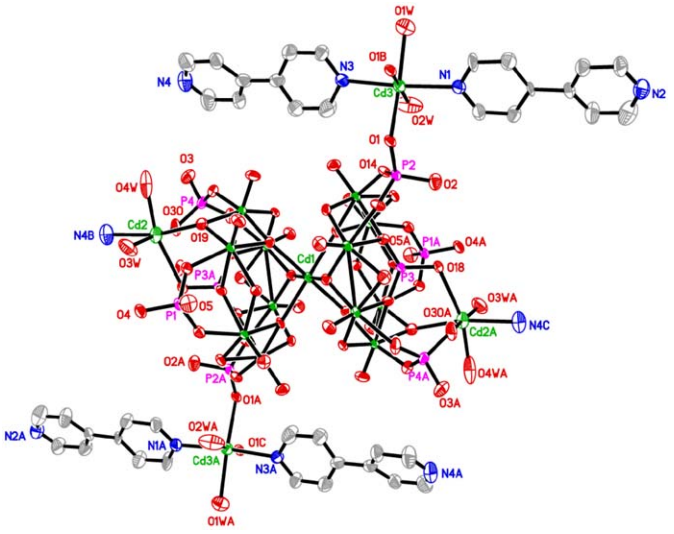

Fig. 1. ORTEP drawing of the basic crystallographic unit in **1** with thermal ellipsoids at 50% probability. Hydrogen atoms are omitted for clarity.

4.4′-bpy molecules, two oxygen atoms (O1 and O1B) of two different $[P_4Mo_6]$ clusters and two water molecules (O1W and O2W).

As shown in Fig. 2a, the Cd(1)$[P_4Mo_6]$ dimers are linked by $[Cd_3(4,4'\text{-Hbpy})_2(4,4'\text{-bpy})_2(H_2O)_8]$ subunits to genrate a plane layer. It is interesting that the infinite plane layers are stacked parallel along *a*-axis to constitute a 3D supramolecular crystal structures, resulting in the formation 1D channel along *a*-axis (Fig. 2b). Free water molecules are located in these channels.

Compound **2** consists of the cations 2D sheets which constructed from $Cd[P_4Mo_6]_2$ dimers linked by $[Cd(4,4'\text{-bpy})(H_2O)]$ complexes, with $[Cd(4,4'\text{-bpy})_3(H_2O)_3]^{2+}$, $Hbpy^+$ and crystal water molecules occupying the interlamellar space. There are three crystallographically independent cadmium ions in compound **2** (shown in Fig. 3). The first one, Cd(1) is located in the $Cd[P_4Mo_6]_2$ dimers and bridges two $[P_4Mo_6]$ units via three μ–O atoms (O25, O28, O23), which link the metal–metal-bonded molybdenum atoms together with Cd–O bond at lengths of 2.205(5) Å × 2, 2.297(5) Å × 2, 2.350(5) Å × 2 to form centrommetric $Cd[P_4Mo_6]_2$ dimers. The second one, Cd(2) is six-coordinate, defined by three oxygen atoms (O6, O8 and O15) from three P–O groups belonging to two different $Cd[P_4Mo_6]_2$ dimers and two nitrogen atoms (N1, N2) from two 4,4′-bpy molecules, as well as a water molecule (O1W). Therefore, the connection of the Cd(1)$[P_4Mo_6]_2$ dimers through $[Cd(2)(4,4'\text{-bpy})(H_2O)]$ complexes produces the layered structure depicted in Fig. 4a. The third one, Cd(3) also has a octahedral environment. It coordinates to three nitrogen atoms from three 4,4′-bpy molecules and three water molecules.

It is interesting that the layers are linked up together to form a 3D supramolecular framework via extensive hydrogen-bonding interactions among the $[P_4Mo_6]$ clusters, free 4,4′-bpy molecules, dissociated $[Cd(4,4'\text{-bpy})_3(H_2O)_3]^{2+}$ complexes and water molecules (see Fig. 4b). The typical hydrogen bonds are N8⋯O30 2.735, N8⋯O9 2.972, O2W⋯O8 2.909, OW1⋯O20 2.706 Å. It is even more interesting that the $[Cd(4,4'\text{-bpy})_3(H_2O)_3]^{2+}$ complexes and the crystal molecules contact each other via hydrogen-bonding interactions to form a 1D chain. Then two adjacent chains are further linked up together to form a 2D supramolecular grid layer through π–π stacking interactions of 4.4′-bpy molecules with the distance of 3.4 Å. The free 4,4′-bpy molecules are located in the grids as shown in Fig. 5. Obviously, these strong hydrogen-bonding interactions and π–π stacking interactions play an important role in the formation of the 3D supramolecular framework.

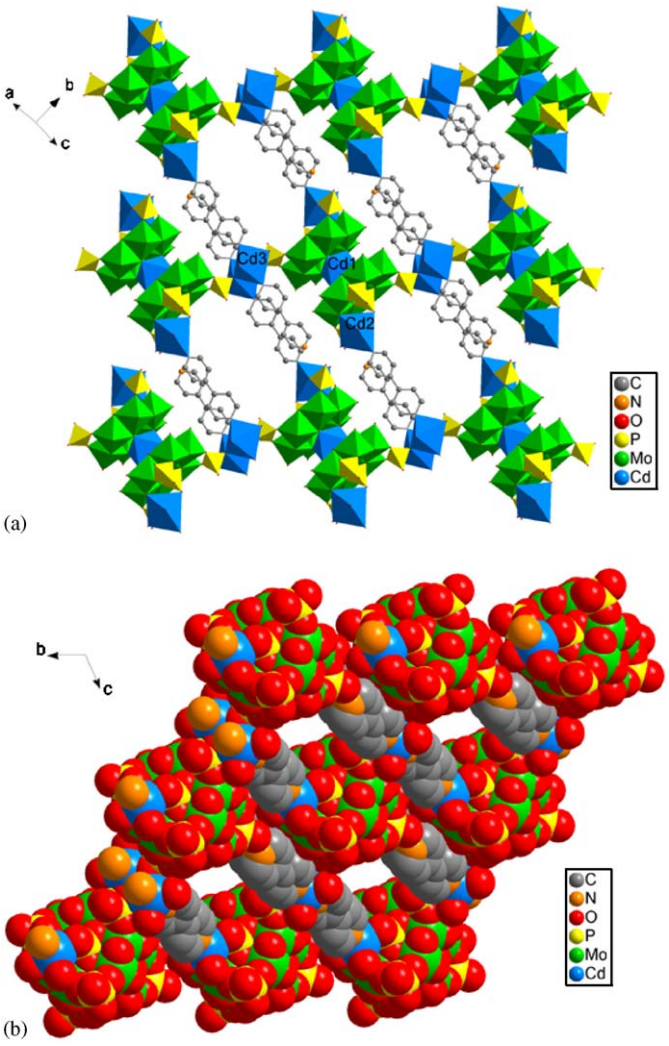

Fig. 2. (a) Polyhedral representation of the 2D layer in **1** and (b) a view along the *a*-axis illustrating the 1D supramolecular channels in **2**.

The structure of compound **3** is a new 2D layered structure which consists of $Cd[P_4Mo_6]_2$ building blocks, tetra-nuclear $[Cd_4(phen)_2(H_2O)_4]$ clusters and $[Cd(phen)(H_2O)]$ complexes. As shown in Fig. 6a, there are four crystallization-independent cadmiums atoms. Cd(1) is located in the $Cd[P_4Mo_6]_2$ dimers and bridges two

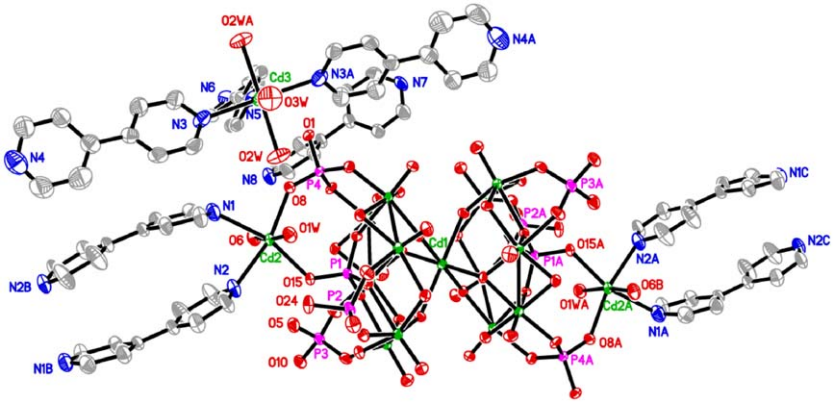

Fig. 3. ORTEP drawing of the basic crystallographic unit in **2** with thermal ellipsoids at 50% probability. Hydrogen atoms are omitted for clarity.

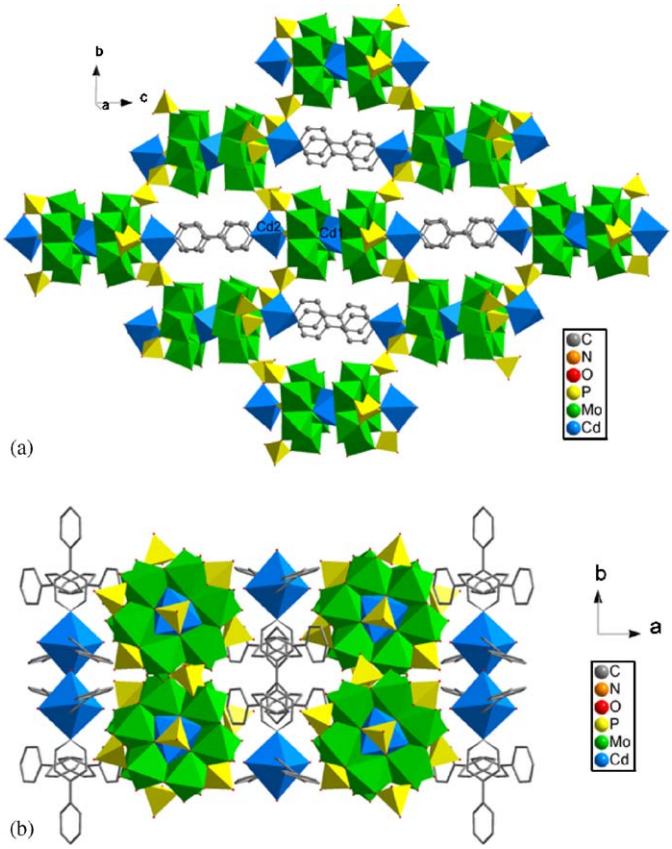

Fig. 4. (a) Polyhedral representation of the 2D layer in **2** and (b) a view along the *c*-axis illustrating the 3D supramolecular framework in **2**.

$[P_4Mo_6]$ units via three μ–O atoms (O2, O13, O9), which link the metal–metal-bonded molybdenum atoms together with Cd–O bond at lengths of 2.276(6) Å × 2, 2.278(7) Å × 2, 2.280(6) Å × 2 to form centrommetric $Cd[P_4Mo_6]_2$ dimers. Cd(2) is six-coordinate, coordinated by four oxygen atoms (O10, O20, O22, O22A) of four P–O groups belonging to two different $Cd[P_4Mo_6]_2$ dimers (where symmetry code A, $-x+1$, $-y-1$, $-z$), an oxygen atom (O1) which linked the metal–metal-bonded molybdenum atoms and a water molecule (O1W). Both Cd(3) and Cd(4) are five-coordinate. Cd(3) is coordinated by two nitrogen atoms (N1, N2) from a phen molecule, an oxygen atom (O10A) of one P–O group and an oxygen atom (O8) which linked the metal–metal-bonded molybdenum atoms from two different $Cd[P_4Mo_6]_2$ dimers, a water molecule (O3W) completes its coordination sphere. It is interesting that the four Cd atoms (Cd3, Cd2B, Cd2, Cd3B) form a centrosymmetrical tetra-nuclear cadmium cluster unit $[Cd_4(phen)_2(H_2O)_4]$ through sharing corner and edge, as shown in Fig. 6b. Cd(4) is coordinated by two nitrogen atoms (N3, N4) from a phen, two oxygen atoms (O12, O29) of two P–O groups from two different $Cd[P_4Mo_6]_2$ dimers and a water molecule (O2W).

As shown in Fig. 7, two adjacent $Cd[P_4Mo_6]_2$ building blocks are linked by tetra-nuclear cadmium clusters $[Cd_4(phen)_2(H_2O)_4]$ to form a 1D chain. Then the two adjacent chains are further contacted each other through the linking of $[Cd(4)(phen)(H_2O)]$ complexes to form a new 2D framework

The structure of compound **4** is similar to that of **3**. It also exhibits 2D framework, in which the $Cd(1)[P_4Mo_6]_2$ dimers are linked by tetra-nuclear cadmium clusters $[Cd_4(2,2'\text{-bpy})_2(H_2O)_4]$ to form a 1D chain, then the two adjacent chains are joined together via the linking of $[Cd(4)(2,2'\text{-bpy})(H_2O)]$ complexes to form a 2D layer (see Fig. 9). Except the organic component is different, the main difference between **3** and **4** is the tetra-nuclear cadmium cluster. As shown in Fig. 8, the tetra-nuclear cadmium cluster in **4** is formed through the sharing of edge instead of the sharing of both corner and edge as in **3**, because the coordinate sphere of Cd3 is changed from 5 in **3** to 6 in **4** (Fig. 9).

The simulated and experimental XPRD patterns of compounds **1**–**4** are shown in Fig. S3. Their peak positions are in good agreement with each other, indicating the phase purity of the products. The differences in intensity may be due to the preferred orientation of the power samples. Meanwhile, the powder XRD patterns for samples of compounds **1**–**4** heated at 100 °C has been done; these are similar to that of the as-synthesized samples, which indicated that the structure was almost maintained after heated at 100 °C.

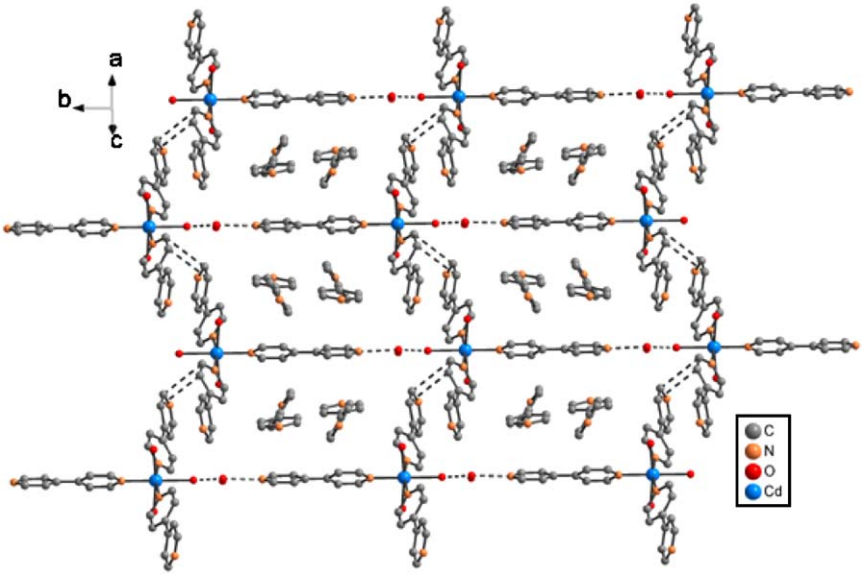

Fig. 5. View of the 2D supramolecular grid layer in **2**.

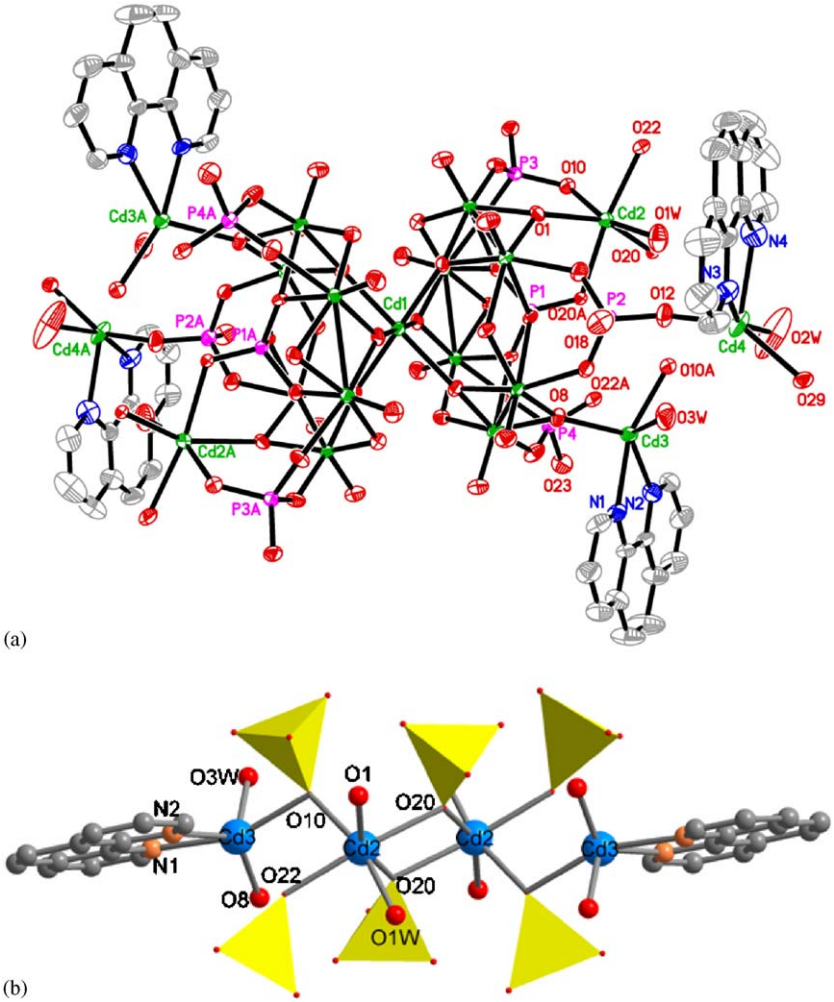

Fig. 6. (a) ORTEP drawing of the basic crystallographic unit in **3** with thermal ellipsoids at 50% probability. Hydrogen atoms are omitted for clarity and (b) view of the tetra-nuclear cadmium cluster $[Cd_4(phen)_2(H_2O)_4]$ in **3** (color code: Cd, blue; P, yellow; O, red; N, orange; C, gray).

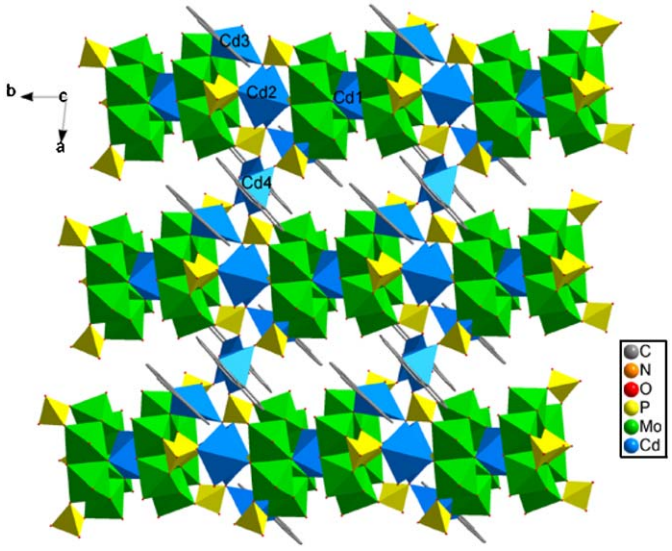

Fig. 7. Polyhedral and ball-stick representation of the 2D framework in **3**.

3.2. IR spectra

The IR spectra of compounds **1** and **2** (Fig. S1a and b) exhibit broad bands at 3320 cm^{-1} (**1**) and 3239 cm^{-1} (**2**) associated with the water molecules. The features at 1610, 1492, 1421 cm^{-1} (**1**) and 1600, 1491, 1417 cm^{-1} (**2**) are assigned to the 4,4′-bpy molecules. The compounds also possess strong bands at 1061, 1018, 967 cm^{-1} (**1**) and 1212, 1106, 1016 cm^{-1} (**2**) attributed to ν(P–O) and strong bands at 967, 806, 742 cm^{-1} (**1**) and 959, 823, 739 cm^{-1} (**2**) attributed to ν(Mo═O) and ν(Mo–O–Mo). In the IR spectra of compounds **3** and **4** (Fig. S1c and d), the broad bands at 3257 cm^{-1} (**3**) and 3309 cm^{-1} (**4**) are associated with the water molecules. The features at 1623, 1518, 1428 cm^{-1} (**3**) and 1633, 1596 and 1440 cm^{-1} (**4**) are assigned to the phen and 2,2′-bpy molecules, respectively. The characteristic peaks at 1143, 1099 and 1040 cm^{-1} (**3**) and 1095 and 1020 cm^{-1} (**4**) are attributed to the ν(P–O) and the characteristic bands at 968, 845, 726 cm^{-1} (**3**) and 970, 762, 736 cm^{-1} (**4**) can be regarded as features of the ν(Mo═O) and ν(Mo–O–Mo) [18,19,21,22].

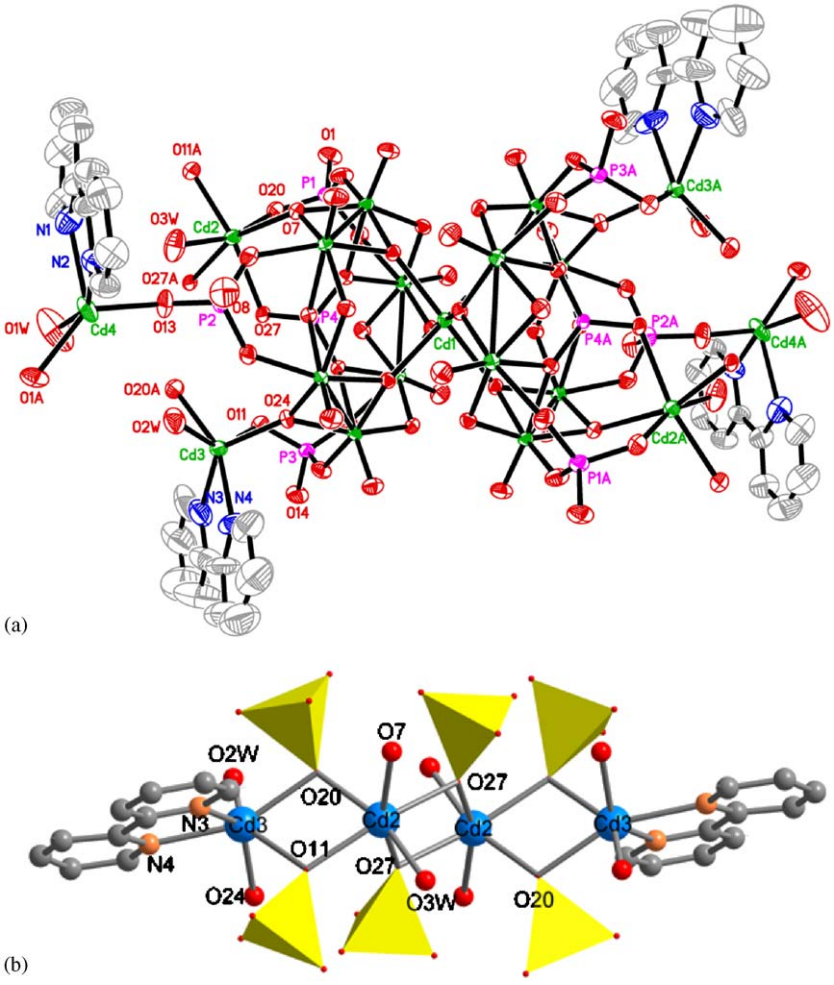

Fig. 8. (a) ORTEP drawing of the basic crystallographic unit in **4** with thermal ellipsoids at 50% probability. Hydrogen atoms are omitted for clarity and (b) view of the tetra-nuclear cadmium cluster $[Cd_4(2,2'\text{-bpy})_2(H_2O)_4]$ in **4** (color code: Cd, blue; P, yellow; O, red; N, orange; C, gray).

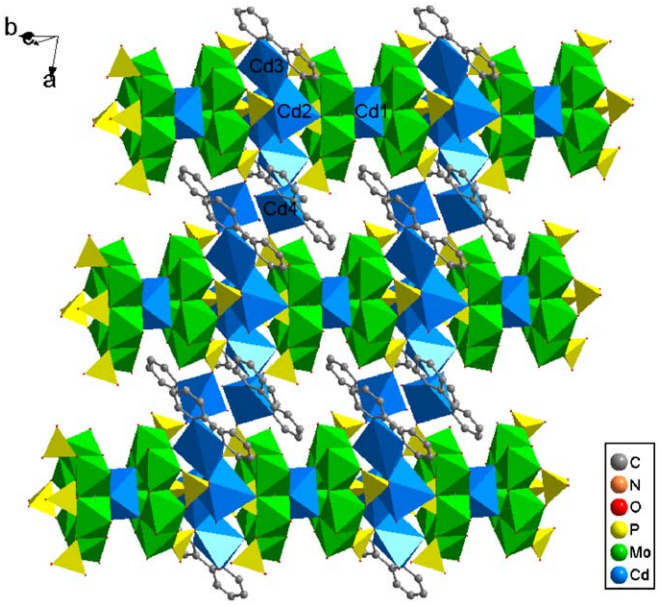

Fig. 9. Polyhedral and ball-stick representation of the 2D framework in **4**.

3.3. Thermal analysis

The TG curve of compound **1** (Fig. S2a) shows that the first weight loss of TG data is 7.06% in the temperature range of 50.65–216.25 °C, corresponding to the loss of crystal and coordinated water molecules (calc. 7.19%). The second weight loss is 16.91% in the temperature range of 239.53–542.02 °C, corresponding to the loss of 4,4′-bpy molecules (calc. 16.64%). The whole weight loss (23.97%) is in agreement with the calculated value (23.83%).

The TG curve of compound **2** (Fig. S2b) exhibits that the first weight loss is 2.62% in the temperature range of 85.83–263.01 °C, corresponding to the loss of crystal and coordinated water molecules (calc. 2.66%). The second weight loss is 26.34% from 297.88 to 527.51 °C, assigned to the loss of 4,4′-bpy molecules (calc. 26.94%). The whole weight loss (28.96%) is in agreement with the calculated value (29.60%).

The TG curve of compound **3** (Fig. S2c) shows that the first weight loss of 3.29% occurred between 40.92 and 219.88 °C, corresponding to the loss of crystal and coordinated water molecules (calc. 3.07%). In the range 390.22–553.81 °C, a second weight loss of 19.56% is observed corresponding to the loss of phen molecules (calc. 19.31%). The whole weight loss (22.85%) is in agreement with the calculated value (22.38%).

The TG curve of compound **4** (Fig. S2d) shows that the first weight loss is 4.24% in the temperature range of 44.61–250.07 °C, corresponding to the loss of crystal and coordinated water molecules (calc. 4.08%). The second weight loss is 15.69% in the temperature range of 356.15–544.46 °C, corresponding to the loss of 2,2′-bpy molecules (calc. 15.72%). The whole weight loss (19.93%) is in agreement with the calculated value (19.80%).

The four compounds continued to lose weight gradually up to 800 °C, the highest temperature measured.

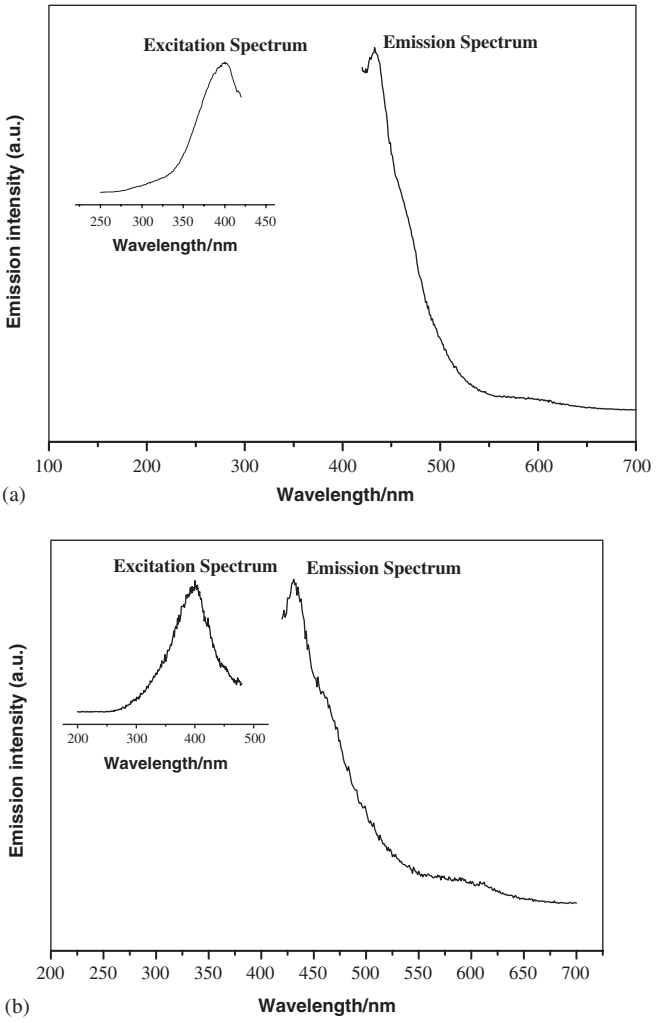

Fig. 10. Solid-state emission spectra of compounds **3** (a) and **4** (b) at room temperature.

3.4. Fluorescent properties of compounds 3 and 4

The solid-state emission spectra of compounds **3** and **4** in room are depicted in Fig. 10. Compound **3** exhibits an intense emission maximum at ca. 433 nm (Fig. 10a, $\lambda_{ex} = 400$ nm). According to previous observations [25], this emission band probably is assigned to the emission of ligand-to-metal charge transfer (LMCT). It can also be observed that an intense emission occurring at 431 nm (Fig. 10b, $\lambda_{ex} = 400$ nm) for **4**. According to the literatures [26], the emission at 431 nm can be assigned to the emission of LMCT. These observations indicate that compounds **3** and **4** may be excellent candidates for potential photoluminescence materials.

4. Conclusions

In this paper, we reported four new $[P_4Mo_6]$ cluster-based extended structures containing cadmium complexes. The success in synthesizing compounds **1**–**4** shows that the $[P_4Mo_6]$ cluster is a versatile building block which not only

can be modified by transitional metal, but also can decorate with transitional metal complexes to construct novel architectures. It is expected to design and synthesize further novel reduced molybdenum phosphates based on $[P_4Mo_6]$ clusters. Furthermore, the fluorescent activities of compounds **3** and **4** may make them to be excellent candidates for potential photoluminescence materials.

5. Supplementary materials

Crystallographic data for the structural analysis have been deposited with the Cambridge Crystallographic Data Center, CCDC reference number: 293063 for **1**, 293064 for **2**, 293065 for **3** and 293066 for **4**. These data can be obtained free of charge at: www.ccdc.cam.ac.uk/conts/retrieving.html (or from the Cambridge Crystallographic Data Center, 12, Union Road, Cambridge CB2 1EZ, UK; fax: +44-1223/336-033; E-mail: deposit@ccdc.cam.ac.uk).

Acknowledgments

This work was financially supported by the National Natural Science Foundation of China (20371011).

Appendix A. Supplementary materials

Supplementary data associated with this article can be found in the online version at: doi:10.1016/j.jssc.2006.04.031.

References

[1] (a) M.T. Pope, Heteropoly and Isopoly Oxometalates, Springer, Berlin, 1983;
(b) C.L. Hill, A. Prosser-McCartha, C.M. Coord, Chem. Rev. 143 (1995) 407;
(c) C.L. Hill, Chem. Rev. 98 (1998) 1.
[2] (a) S.T. Zheng, J. Zhang, G.Y. Yang, Inorg. Chem. 44 (2005) 2426;
(b) M.I. Khan, E. Yohannes, R.J. Doedens, Inorg. Chem. 42 (2003) 3125;
(c) B.Z. Lin, S.X. Liu, J. Chem. Soc. Chem. Commun. (2002) 2126;
(d) C.M. Liu, D.Q. Zhang, M. Xiong, D.B. Zhu, J. Chem. Soc. Chem. Commun. (2002) 416;
(e) Y. Lu, Y. Xu, E.B. Wang, J. Lü, C.W. Hu, L. Xu, Cryst. Growth Des. 5 (2005) 257;
(f) P.J. Zapf, C.J. Warren, R.C. Haushalter, J. Zubieta, J. Chem. Soc. Chem. Commun. (1997) 1543;
(g) V. Shivaish, M. Nagaraju, S.K. Das, Inorg. Chem. 42 (2003) 6604.
[3] (a) C.Z. Lu, C.D. Wu, H.H. Zhuang, J.S. Huang, Chem. Mater. 14 (2002) 2649;
(b) D. Hagrman, C. Zubieta, D.J. Rose, J. Zubieta, R.C. Haushalter, Angew. Chem. Int. Ed 36 (1997) 873;
(c) W.B. Yang, C.Z. Lu, H.H. Zhuang, J. Chem. Soc. Dalton Trans. 14 (2002) 2879;
(d) D. Hagrman, C. Sangregorio, C.J. O'Connor, J. Zubieta, J. Chem. Soc. Dalton Trans. (1998) 3707.
[4] R.C. Haushalter, L.A. Mundi, Chem. Mater. 4 (1992) 31.
[5] S.T. Wang, E.B. Wang, Y. Hou, Y.G. Li, L. Wang, M. Yuan, C.W. Hu, Transition Met. Chem. 28 (2003) 616.
[6] A. Leclaire, C. Biot, H. Rebbah, M.M. Borel, B. Raveau, J. Mater. Chem. 8 (1998) 439.
[7] Y.S. Zhou, L.J. Zhang, X.Z. You, S. Natarajan, Inorg. Chem. Commun. 4 (2001) 299.
[8] Y.S. Zhou, L.J. Zhang, H.K. Fun, New J. Chem. 25 (2001) 1342.
[9] C. du Peloux, P. Mialane, A. Dolbecq, J. Marrot, F. Varret, F. Sécheresse, Solid State Sci. 6 (2004) 719.
[10] L.A. Meyer, R.C. Haushalter, Inorg. Chem. 32 (1993) 1579.
[11] C. du Peloux, P. Mialane, A. Dolbecq, J. Marrot, E. Rivière, F. Sécheresse, J. Mater. Chem. 11 (2001) 3392.
[12] Y.H. Sun, X.B. Cui, J.Q. Xu, L. Ye, Y. Li, J. Lu, H. Ding, H.Y. Bie, J. Solid State Chem. 177 (2004) 1811.
[13] H.X. Guo, S.X. Liu, J. Mol. Struct. 741 (2005) 229.
[14] L. Xu, Y.Q. Sun, E.B. Wang, E.H. Shen, Z.R. Liu, C.W. Hu, New J. Chem. 23 (1999) 533.
[15] L. Xu, Y.Q. Sun, E.B. Wang, E.H. Shen, Z.R. Liu, C.W. Hu, J. Solid State Chem. 146 (1999) 533.
[16] L. Xu, Y.Q. Sun, E.B. Wang, E.H. Shen, Z.R. Liu, C.W. Hu, Y. Xing, Y.H. Lin, H.Q. Jia, Inorg. Chem. Commun. 1 (1998) 382.
[17] R.D. Huang, F.C. Liu, Y.G. Li, M. Yuan, E.B. Wang, G.J.H. De, C.W. Hu, N.H. Hu, H.Q. Jia, Inorg. Chim. Acta 349 (2003) 85.
[18] M. Yuan, E.B. Wang, Y. Lu, Y.G. Li, C.W. Hu, N.H. Hu, H.Q. Jia, Inorg. Chem. Commun. 5 (2002) 505.
[19] M. Yuan, E.B. Wang, Y. Lu, Y.G. Li, C.W. Hu, N.H. Hu, H.Q. Jia, J. Solid State Chem. 170 (2003) 192.
[20] L.A. Mundi, R.C. Haushalter, Inorg. Chem. 31 (1992) 3050.
[21] H.X. Guo, S.X. Liu, J. Mol. Struct. 751 (2005) 156.
[22] (a) L.Y. Duan, F.C. Liu, X.L. Wang, E.B. Wang, C. Qin, Y.G. Li, X.L. Wang, C.W. Hu, J. Mol. Struct. 705 (2004) 15;
(b) H.X. Guo, S.X. Liu, Inorg. Chem. Commun. 7 (2004) 1217.
[23] (a) G.M. Sheldrick, SHELX 97, Program for Crystal Structures Refinement, University of Göttingen, Germany, 1997;
(b) G.M. Sheldrick, SHELX 97, Program for Crystal Structures Solution, University of Göttingen, Germany, 1997.
[24] I.D. Brown, D. Altermatt, Acta Cryst. B 41 (1985) 244.
[25] (a) K.D. Ley, K.S. Schanze, Coord. Chem. Rev. 171 (1998) 287;
(b) V.W.W. Yan, K.K.W. Lo, Chem. Soc. Rev. 28 (1999) 323.
[26] (a) N. Hao, E.H. Shen, Y.G. Li, E.B. Wang, C.W. Hu, L. Xu, Eur. J. Inorg. Chem. (2004) 4102;
(b) C. Qin, X.L. Wang, E.B. Wang, L. Xu, J. Mol. Struct. 738 (2005) 91.